IOP Conf. Series: Materials Science and Engineering **370** (2018) 012054 doi:10.1088/1757-899X/370/1/012054

A qualitative study of vortex trapping capability for lift enhancement on unconventional wing

M B Salleh[a)], N M Kamaruddin[b)] and Z Mohamed-Kassim[c)]

School of Aerospace Engineering, Engineering Campus, Universiti Sains Malaysia, 14300 Nibong Tebal, Penang, Malaysia

[b)] Corresponding author: fazreena@usm.my

Abstract. Lift enhancement by using passive vortex trapping technique offers great advantage in small aircraft design as it can improve aerodynamics performance and reduce weight of the wing. To achieve this aim, a qualitative study on the flow structures across wing models with cavities has been performed using smoke wire visualisation technique. An experiment has been conducted at low Reynolds number of 26,000 with angle of attack (α) = 0°, 5°, 10° and 15° to investigate the vortex trapping capability of semi-circular leading edge (SCLE) flat-plate wing model and elliptical leading edge (ELE) flat-plate wing model with cavities, respectively. Results from the qualitative study indicated unique characteristics in the flow structures between the tested wing models. The SCLE wing models were able to trap stable rotating vortices for $\alpha \leq 10°$ whereas the ability of ELE wing models to suppress flow separation allowed stable clockwise vortices to be trapped inside the cavities even at $\alpha > 10°$. The trapped vortices found to have the potential to increase lift on the unconventional wing models.

1. Introduction

The capability to enhance lift generation and to delay flow separation on a wing can improve the aircraft aerodynamic performance. Many studies have been conducted to increase the performance particularly its lift-to-drag ratio by using a flow control technique across the wing which can be classified as active or passive flow control techniques. For instance, the active flow control techniques use high lift devices such as flaps or slats which can be installed on the wing. During take-off, the aircraft would extend these control surface devices to achieve an additional camber effect which would augment the lift [1]. The drawback of this active lift augmentation system, however, it adds substantial weight, complexity and manufacturing cost. Another alternative active control technique is by using power driven streamwise, tangential blowing and suction system [2]-[4]. This technique is mostly effective in the post-stall regime where a slot suction is introduced inside the trailing edge vortex cell of a thick airfoil [5][6]. However, the presence of the slot suction complicates the wing structure design.

Another reliable method to increase the lift is through the usage of passive trapped vortex. Ringleb [7] discovered this technique by introducing vortex cavities on the wing. The technique has proven to potentially delay the flow separation and promote the flow reattachment which can be associated to lift enhancement. Unlike active flow control, passive flow control technique does not require auxiliary power to operate any active mechanisms. The presence of cavities on the wing surface helps to reduce

the weight of the wing. Therefore, this technique is favorable to be implemented on a small size aircraft such as an Unmanned Aerial Vehicles (UAVs) and Micro Aerial Vehicles (MAVs). Considering the requirements of having high performance aircraft under power and weight constraints, there is a growing number of research that focus on the study of vortex trapping for lift enhancement.

Yeung [8] has studied vortex trapping technique through numerical approach by using a conformal mapping sequence to explore the ability of an airfoil to trap a single and multiple vortices inside the cavities. In his study, the Joukowsky airfoil with a single cavity, two cavities and three cavities were investigated. Based on the numerical analysis, he concluded that the Joukowsky airfoil with the triple cavities can generate lift 10% higher than the conventional Joukowsky airfoil with the same thickness, camber and angle of attack. The trapped vortices were found to be rotated in a closed elliptical path. Meanwhile, Olsman and Colinius [9] conducted two dimensional direct numerical simulation of the flow across NACA 0018 airfoil without and with cavity at Reynolds number, $Re = 20{,}000$. The results of the study showed that the airfoil with a cavity produced a smaller wake as compared to the airfoil without any cavity at angle of attack $\alpha = 10°$.

Meanwhile, Fertis et al. [10] conducted an experimental study on a new airfoil design with a backward-facing steps. They found that the airfoil can increase the lift-to-drag ratio by 28% at $\alpha = 10°$ due to the trapped vortex. Then, Riddle et al. [5] performed similar flow visualization experiment by using a water channel to study the vortex trapping techniques. In their study, two airfoil designs were considered, one with a backward-facing step configuration and the other one with a dual-fence configuration. The dual-fence configuration was found to be more effective in trapping vortex than the backward-facing step as it requires low suction rates. Araque and Nožicka [11] conducted flow visualization study on an NACA 2415 airfoil with a backward-facing step using smoke wire technique. The double-coiled Nichrome wire coated with liquid glycerine produced a clear and distinct smoke streaklines and the results agreed well with the numerical simulation conducted by Araque [12].In addition, a three dimensional instability was also identified through experimental investigations. For instance, Savelsberg and Castro [13] studied the flow inside a large aspect ratio cylindrical vortex cell. They found that the flow in the cavity which was driven by a shear layer forming in the opening showed a nearly solid body rotation, with a low turbulence layer forming in the vortex core. Tee [14] adopted smoke wire technique of Araque and Nožicka [11] to collect a physical evidence of trapped vortex inside the cavity of NACA 0018 wing model. A flat plate wing models with different number of cavity were also tested as a fundamental study. From the experiment, it was found that the blunt semi-circular leading edge nose of the flat plate wing model caused the flow to separate earlier at the leading edge thus resulting in an unstable vortex formation inside the wing model with three cavities. It has been suggested that slender elliptical leading edge nose could potentially delay the flow separation and hence promote stable vortices inside the cavities.

In this paper, the qualitative study on vortex trapping capability technique for unconventional wing models conducted by Tee [14] is further extended by considering two different types of flat plate wing model with cavities i.e. (i) semi-circular leading edge (SCLE) wing model and (ii) elliptical leading edge (ELE) wing model. To simulate a small size aircraft (MAV and UAV) flying condition, wing models were tested under the same low Reynolds number of 26,000 inside a closed-circuit wind tunnel facility. A qualitative approach by using the smoke wire visualization technique was utilized to study the flow structure across the wing models and the dynamic of trapped vortex inside the cavity. At first, the study focuses at the vortex trapping capability of the SCLE wing model at angle of attack $\alpha = 0°$, 5°, 10° and 15° then followed by the ELE wing models for the same angle of attacks. The results obtained for all tested wing models are discussed in term of the capability of the wing models to trap the vortex inside the cavities at different angle of attack with respect to the type of the wing model.

2. Experimental Setup

2.1 Wind tunnel facility

The experiments have been conducted in a closed-circuit wind tunnel at the Wind Tunnel Laboratory, Science and Engineering Research Centre (SERC), Universiti Sains Malaysia. The wind tunnel has a rectangular test section of 1.0 m (width) × 0.8 m (height) × 1.8 m (length), a contraction ratio of 10:1 and a turbulence level of 0.1%. Airflow inside the test section can achieve a maximum speed of 80 m/s and it is recirculated by an axial fan motor and a diffuser downstream the test section. In addition, the test section is equipped with an internal balance mounted on a quadrant mechanism which has the capability to change the angle of attack of the wing models.

2.2 Smoke wire visualization technique

The airflow structures across the wing models have been visualized by using a smoke wire technique, as shown in Figure 1. For this setup, a single Nichrome wire with a diameter of 0.25 mm has been used to generate clear and distinct smoke lines. This wire has been placed vertically upstream with respect to the tested wing models, 0.57 m from the leading edge of SCLE wing model (equivalent to 0.47 m from the leading edge of ELE wing model) and 4.5 cm inbound of the wingtip to provide clear images of the flow structures across the wing models. Electric current were used to heat up the wire by connecting the positive and negative terminal at both end of the wire by using some crocodile clips. A direct current (DC) power supply of 31 V and 1.2 A were used to supply the electrical current across the wire. The smokes were generated when the oil dripping down the heated Nichrome wire evaporated. For the source of smoke, Safex oil has been used due to its non-toxicity. The oil was dripped down through the wire manually from the top of the wind tunnel test section by using a syringe. Since the smokes are white, the top and rear backgrounds of test section have been covered with a black sugar paper to increase the contrast and to avoid any reflection of light source from the surrounding. In order to capture clear images, the smoke streak lines have been illuminated with four parabolic white reflector halogen lamps, with each two were installed at the top and bottom of the test section, respectively.

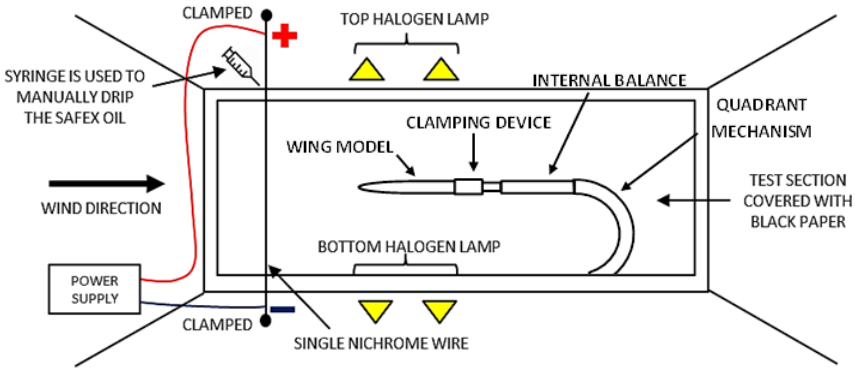

Figure 1. Smoke wire visualization setup.

2.3 Wing models

Two types of wing models were considered in this study, distinguished by the shape of the leading edge nose (i) semi-circular leading edge (SCLE) flat-plate wing model and (ii) elliptical leading edge (ELE) flat-plate wing model, as shown in Figure 2. These wing models have the same thickness of 0.03 m and wing span of 0.5 m. The SCLE wing model has a chord length of 0.25 m which gives the aspect ratio of the wing AR = 2 whereas the ELE wing model has a chord length of 0.35 m which give the aspect ratio AR = 1.43. Both wing models have three cavities of the same size on the upper surface where the dimension of the cavities is adopted from Yeung [8]. In addition, the wing models have

holes at the mid-section of the trailing edge to accommodate for the clamping device. All wing models were painted in matte black to reduce the light reflection during experiment.

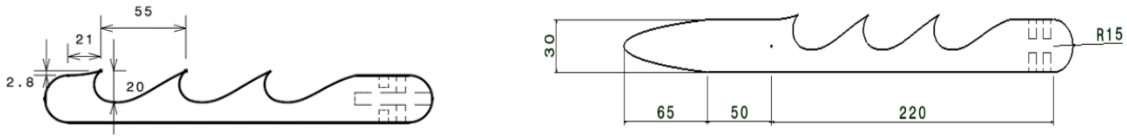

(a) (b)

Figure 2. Cross section views of (a) SCLE wing model with three cavities and (b) ELE wing model with three cavities. Units are shown in millimeters (mm).

2.4 Experimental procedure

The wing model was mounted on the internal balance by using a clamping device and its initial angle of attack was set at 0° by using a digital inclinometer. Then, the qualitative study on the flow structures across each wing model was performed at Reynolds number Re = 26,000 for an angle of attack α = 0°, 5°, 10° and 15°, respectively. First, the experiment was performed for the SCLE wing models then followed by the ELE wing models. Since the SCLE and ELE wing models were different in chord length, the airspeed was set at 1.5 m/s for the SCLE wing models whereas for the ELE wing models, the air speed was set at 1.1 m/s corresponding to the similar Reynolds number. A video camera with a resolution of 1920 × 1080i and 30 frames per second (fps) was employed to acquire the images of the airflow structure across the wing models. The camera was placed outside of the test section and located perpendicular to the smoke streak lines, as shown in Figure 3. A black cloth was used to cover the camera during recording process to reduce any external light disturbance. The images of the airflow structure across the wing models were recorded and all acquired images were then analyzed.

Figure 3. A camera was mounted on the tripod stand outside the test section. A black cloth was used to cover the camera to reduce light disturbance from the surrounding.

3. Results

This section presents and discusses the smoke flow visualization of the flow structures across the wing models at different angle of attack, respectively. The experimental results are discussed in terms of the flow structures across the tested wing models and the dynamics of trapped vortices inside the cavities.

In addition, the comparison on the flow structures and capability to trap vortex in the cavity between SCLE and ELE wing models is also discussed. Note that the flow direction of the smoke streak lines presented in the following figures is from left to right.

The airflow dynamics across the SCLE wing model with triple cavities at different angle of attack are shown in Figure 4. At $\alpha = 0°$ as depicted in Figure 4(a), the flow remains attached across the wing model with a stagnation point located at the leading edge nose. The flow right above the first and the second cavity was captured into the cavities to form a clockwise vortex. There was also a vortex trapped inside the third cavity which was formed when the flow structures inside the second cavity escaped and then entered the third cavity. The trajectory momentum and intensity of the vortex flow inside the second cavity was observed to be more distinct than the vortex inside the first cavity which suggests the capability of the trapped vortex to escape the second cavity. Meanwhile, vortex formation was observed in all cavities at $\alpha = 5°$, as shown in Figure 4(b). The trapped vortex inside the first and second cavity was circulating in a clockwise direction and formed as the freestream flow entered the cavities. The intensity of the vortex inside the first cavity was much more distinct than the inside of the second cavity and sufficient to induce flow reattachment downstream the leading edge nose. As the freestream flow above the cavities was sucked in at the cavity trailing edge, it can be deduced that all trapped vortex inside the cavities rotated in a clockwise direction. At $\alpha = 0°$ and 5°, however, the vortex inside the cavities only trapped at the top portion of the cavity. As the angle of attack increased to $\alpha = 10°$ in Figure 4(c), the flow separated earlier at the trailing edge of the wing model and no distinct vortex was found to be trapped inside the first cavity. Moreover, unstable vortex formations were observed inside the second and third cavity which came from the wingtip vortex. These trapped vortex were observed to be turbulent in motion which hindered the flow reattachment to occur. At $\alpha = 15°$, the airflow across the wing model was completely separated, as depicted in Figure 4(d). There was no trapped vortex from the freestream in any cavities except the wingtip vortex that entered the second and third cavity. Based on the results, it can be deduced that the tested SCLE wing model with three cavities was more reliable to trap vortex at a small range of angle of attack. In this range, a stable clockwise rotating vortex can only be captured inside the first and the second cavity. Inside the third cavity, however, the flow structure was turbulent that formed from the wingtip vortex which becomes more prominent as the angle of attack increases.

Figure 5 shows the airflow structures across the ELE wing model with three cavities. At $\alpha = 0°$ the stagnation point was located exactly at the tip of the leading edge nose of the wing model and the flow remained attached on the wing surface. There was a vortex trapped inside the first cavity and it was rotated in a clockwise motion, as shown in Figure 5(a). Unlike the vortex inside the cavities of the SCLE wing model which was trapped only at the top portion of the cavity, the vortex inside the first cavity of the ELE wing model had covered the whole space of cavity thus forming a stable flow structure. Moreover, the intensity of the vortex was distinct than the vortex in the SCLE wing model which suggests that a stronger vortex with a higher momentum was trapped inside the cavity. The clockwise circulation of the vortex inside the first cavity also kept the freestream flow to remain attached towards the trailing edge of the wing model. Detailed observation found that there was a flow injected into the second cavity but the trapped vortex inside this cavity was very weak whereas there was no vortex observed inside the third cavity. Similar flow structures were observed at $\alpha = 5°$ where there was a clear and distinct clockwise vortex trapped inside the first cavity, as shown in Figure 5(b). A faint and weak vortex can also be observed inside the third cavity and it was formed as the wingtip vortex entered the cavity.

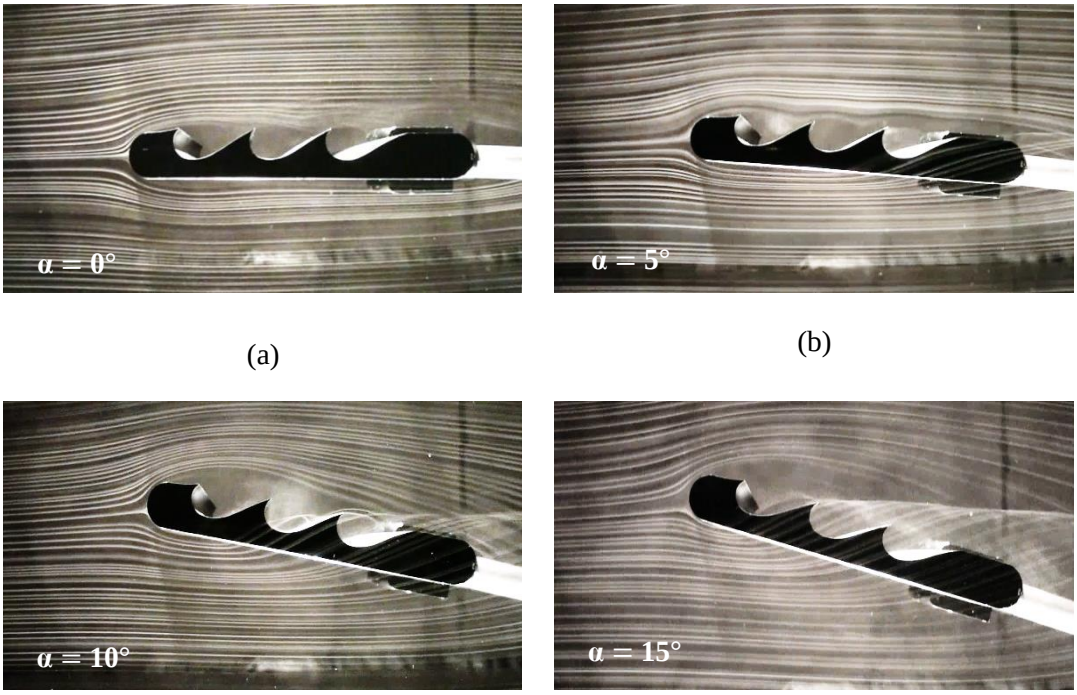

Figure 4. Airflow structures across the SCLE wing model with three cavities.

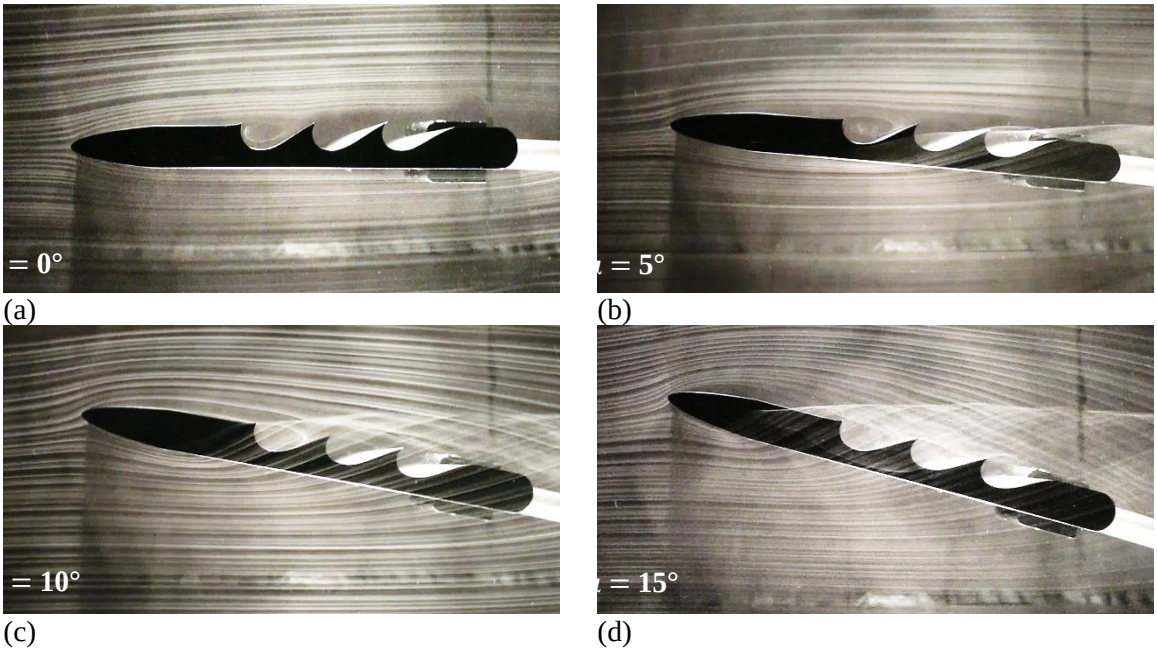

Figure 5. Flow structures at tested angle of attacks for ELE wing model with triple cavities.

For α = 10° a vortex was successfully trapped by the first cavity, as shown in Figure 5(c). The trapped vortex has the similar trajectory strength and as distinct as the case of α = 0° and 5°. The trapped vortex was observed to circulate in a clockwise motion and promoted consistent flow reattachment after the trailing edge of first cavity. In addition, there was a trapped vortex inside the second cavity.

Unlike for the case of SCLE wing model, this vortex was formed as the freestream flow engulfed into the second cavity. However, it has less prominent flow structure as compared to the vortex inside the first cavity thus failed to induce a proper flow reattachment at the trailing edge of the second cavity. This situation caused the freestream flow to slightly fluctuate over the third cavity downstream of the trailing edge of the wing model thus no vortex was observed inside the third cavity. When the wing model was pitched to $\alpha = 15°$, the airflow separated after the leading edge nose but reattached again as it flowed pass the leading edge nose and across the wing model, as depicted in Figure 5(d). It was observed that the shear layer entered the cavities to form a clockwise vortex. Although the intensity of the wingtip vortex grew greater and became more prominent, the trapped vortex inside the cavities was observed to be dominated by the incoming freestream flow above the cavities. The trapped vortex has the capability to successfully promote flow reattachment at the trailing edge of each cavity thus suppressing the flow separation downstream the wing model even at high angle of attack.

4. Conclusion

The vortex trapping capability across two different types of wing models with three cavities have been qualitatively studied using the smoke wire visualization technique. The experiments have been conducted to investigate the characteristic of the flow structures on the upper surface of the wing with the present of cavities. The results have revealed that the flow structures across the wing models were affected by the shape of the leading edge nose. The blunt leading edge nose of SCLE wing model caused the freestream flow to separate at high angle of attack. In contrast, with a slender leading edge nose, the ELE wing model successfully suppressed the flow separation for the tested angle of attacks thus increased the stall angle of the wing. As a result, the SCLE wing models with cavities only able to trap stable clockwise vortex for $\alpha \leq 10°$. These stable vortex were normally found to be trapped inside the first and second cavity whereas the vortex trapped inside the third cavity was unstable and formed as the wingtip vortex entered the cavity. Meanwhile, the ELE wing model was able to trap a stable clockwise vortex inside all cavities. The vortex trapped inside the cavities were found to be more stable and distinct than that of SCLE wing model with less influence from the wing tip vortex even at higher angle of attack $\alpha > 10°$. The trapped clockwise vortex inside the cavities for both wing models have the capability to enhance lift proven by the clockwise motion configuration.

Acknowledgements

The authors acknowledge financial support from Universiti Sains Malaysia, wing model designs and experimental setup assisted by Mr Tham Weng Hong, Ms. Tey Shen Xi, Ms. Tee Yi Hui, Mr. Anuar M Nazri and technical supports from Mr Mohamad Najhan Awang and Mr Mahmud Isa from School of Aerospace Engineering USM.

References

[1] Yeung W W H 2009 Vortex trapping on a surface with an indentation and corrugations *Mathematics and Computers in Simulation*, **79**, pp 3243–57.

[2] Baranov P A, Isaev S A, Prigorodov Y S and Sudakov A G 1999 Numerical modelling of the effect of improving the aerodynamic efficiency of profiles due to the suction in vortex cells *J. of Eng. Physics and Thermophysics* **72** pp 550–53

[3] Baranov P A, Isaev S A, Prigorodov Y S and Sudakov A G 2003 Controlling the turbulent flow past a thick airfoil by means of flow enhancement in a vortex cell using suction from central body surfaces *Fluid Dynamics* **38** pp 387–96

[4] Isaev S A, Miau J J, Sudakov A G and Usachov A E 2015 Analysis of extremal lift behavior of a semicircular airfoil in a turbulent flow at a near-zero angle of attack *Technical Physics Letters* **41** pp 737–39

[5] Riddle T W, Wadcock A J, Tso J and Cummings R M 1999 An Experimental Analysis of Vortex Trapping Techniques *J.of Fluids Engineering* **121** pp 555-59

[6] Isaev S, Baranov P, Popov I, Sudakov A and Usachov 2016 A Improvement of Aerodynamic Characteristics of a Thick Airfoil with a Vortex Cell in Sub- and Transonic Flow *Acta Astronautica* **132** pp 204-20
[7] Ringleb F O 1961 *Boundary Layer Flow Control Device* US Patent 3,000,40
[8] Yeung W W H 2006 Lift Enhancement of Unconventional Airfoils *J. Mekanikal*, **79**, pp 17-25
[9] Olsman W F J and Colonius T 2011 Numerical Simulation of Flow over an Airfoil with a Cavity *AIAA JOURNAL* **49** No. 1 pp 143-149
[10] Fertis D G 1994 New Airfoil Design Concept with Improved Aerodynamic Characteristics," *J. of Aerospace Eng.* **7** No. 3 pp 328-39
[11] Araque L. V- and Nožicka J 2011 Oil And Smoke Flow Visualization Past Two-Dimensional Airfoils For An Unmanned Aerial Vehicle *Visualization of Mechanical Processes* **1** (3) pp 1-8
[12] Araque L V- 2010 Development of an Airfoil for an Unmanned Aerial Vehicle with Internal Blowing Propulsion System *Ph.D Thesis* Czech Technical University in Prague
[13] Savelsberg R and Castro I 2008 Vortex Flows in Open Cylindrical-Section Cavities *Exp. Fluids* **46** (3) pp 485-97
[14] Tee H Y 2015 Development of Smoke Wire System for Vortex Trapping Application, *Final Year Project Thesis* Universiti Sains Malaysia